


**RESEARCH ARTICLE**

# Effects of cell seeding technique and cell density on BMP-2 production in transduced human mesenchymal stem cells

Kevin Collon<sup>1</sup>  | Jennifer A. Bell<sup>1</sup> | Stephanie W. Chang<sup>1</sup> | Matthew C. Gallo<sup>1</sup> | Osamu Sugiyama<sup>1</sup> | Carolyn Marks<sup>2</sup> | Jay R. Lieberman<sup>1</sup>

<sup>1</sup>Department of Orthopaedic Surgery, Keck School of Medicine of USC, Los Angeles, California, USA

<sup>2</sup>Core Center of Excellence in Nano Imaging, University of Southern California, Los Angeles, California, USA

**Correspondence**

Kevin Collon, Department of Orthopaedics, Keck Medical Center of USC, 1520 San Pablo St, Suite 2000, Los Angeles, CA 90033, USA.  
Email: [kevin.collon@med.usc.edu](mailto:kevin.collon@med.usc.edu)

**Abstract**

Small animal models have demonstrated the efficacy of ex vivo regional gene therapy using scaffolds loaded with BMP-2-expressing mesenchymal stem cells (MSCs). Prior to clinical translation, optimization of seeding techniques of the transduced cells will be important to minimize time and resource expenditure, while maximizing cell delivery and BMP-2 production. No prior studies have investigated cell-seeding techniques in the setting of transduced cells for gene therapy applications. Using BMP-2-expressing transduced adipose-derived MSCs and a porous ceramic scaffold, this study compared previously described static and dynamic seeding techniques with respect to cell seeding efficiency, uniformity of cell distribution, and in vitro BMP-2 production. Static and negative pressure seeding techniques demonstrated the highest seeding efficiency, while orbital shaking was associated with the greatest increases in BMP-2 production *per cell*. Low density cell suspensions were associated with the highest seeding efficiency and uniformity of cell distribution, and the greatest increases in BMP-2 production from 2 to 7 days after seeding. Our results highlight the potential for development of an optimized cell density and seeding technique that could greatly reduce the number of MSCs needed to produce therapeutic BMP-2 levels in clinical situations. Further studies are needed to investigate in vivo effects of cell seeding techniques on bone healing.

**KEYWORDS**

bone repair, gene therapy, mesenchymal stem cell, scaffold, tissue engineering

## 1 | INTRODUCTION

The reconstruction of large bone defects poses a significant challenge in the field of Orthopedic Surgery. While many therapeutic approaches exist for the management of bone loss, bone autograft remains the gold standard as it provides all three elements required for bone repair: an osteoinductive stimulus, osteogenic cells, and an osteoconductive scaffold.<sup>1,2</sup> However, autograft is limited in quantity and is associated with significant harvest site morbidity.<sup>3,4</sup> Bone

tissue engineering strategies provide an exciting potential alternative for developing effective, low-morbidity treatment options for reconstruction of large bone defects in a wide range of patients.

One approach to tissue engineering for bone repair is ex vivo regional gene therapy. Osteogenic stem cells are isolated from a tissue sample and expanded in culture. The cells are then genetically modified to express an osteoinductive stimulus such as bone morphogenetic protein 2 (BMP-2). The transduced cells are seeded onto a porous 3D scaffold and implanted into a bone defect, providing all

This is an open access article under the terms of the [Creative Commons Attribution-NonCommercial-NoDerivs](https://creativecommons.org/licenses/by-nc-nd/4.0/) License, which permits use and distribution in any medium, provided the original work is properly cited, the use is non-commercial and no modifications or adaptations are made.

© 2022 The Authors. *Journal of Biomedical Materials Research Part A* published by Wiley Periodicals LLC.

three elements required for bone repair. A potential advantage of *ex vivo* regional gene therapy is that the cells provide a sustained osteoinductive stimulus (i.e., weeks to months) during bone repair and remodeling. In preclinical critical sized femoral defect models, consistent and robust bone repair has been demonstrated using *ex vivo* regional gene therapy.<sup>5-7</sup>

Seeding cells onto a scaffold prior to implantation is a critical step in *ex vivo* regional gene therapy, or in any cell-based tissue engineering approach, as it determines the number of cells delivered and retained at the defect site to exert a therapeutic effect.<sup>8</sup> In addition to cell number, the distribution of cells throughout the 3D volume of the scaffold has been shown to have an impact on cell viability, migration, differentiation, and the architecture of bone tissue formation.<sup>9,10</sup>

For these reasons, optimization of cell seeding methods has previously been evaluated in a broad range of porous scaffold materials, including calcium phosphate ceramics. An optimized cell seeding method should be time efficient, minimize cell loss, and achieve homogeneous cell distribution throughout the scaffold, the latter of which has been shown to promote functional tissue development.<sup>11</sup> Broadly, seeding methods can be classified as either static or dynamic.<sup>12</sup> Examples of static seeding methods include the “soak” method, in which a scaffold is placed directly into a cell suspension, or the more commonly used method whereby a cell suspension is loaded onto a scaffold using a standard pipette.<sup>8,13</sup> Dynamic seeding methods seed cells in the presence of kinetic forces such as continuous perfusion, shaking, or negative pressure.<sup>8,12,14</sup> Dynamic seeding methods are generally seen as superior because they tend to result in a more homogeneous cell distribution and the cells have greater access to nutrients during seeding. Multiple studies have concluded that dynamically seeded mesenchymal stem cells also have enhanced osteogenic potential, and that the mechanical stimulation associated with dynamic culturing conditions has a significant impact on cell differentiation and gene expression.<sup>13,15,16</sup> However, these studies have been exclusively performed in non-transduced cells. The question remains whether dynamic seeding methods might also influence transgene expression in transduced MSCs intended for use in *ex vivo* gene therapy. Dynamic seeding methods that also enhance osteoinductive transgene expression have the potential to dramatically improve the efficiency of cell seeding on a scaffold, which can reduce the cell dose needed for treatment. This could reduce costs associated with cell culture, expansion, and transduction for the clinical application of *ex vivo* regional gene therapy techniques for bone repair.

The purpose of this study was to evaluate the effects of previously described static (pipetting) and dynamic (negative pressure and orbital shaker) cell seeding methods, at various cell densities, on seeding efficiency, cell distribution, and BMP-2 expression with human adipose-derived mesenchymal stem cells (ASCs) transduced to over-express BMP-2 and seeded onto a porous ceramic scaffold. We hypothesized that dynamic seeding methods would be associated with a higher seeding efficiency, more homogenous cell distribution, and subsequently higher levels of BMP-2 production.

## 2 | METHODS

### 2.1 | Cell harvest

Institutional Review Board approval was obtained prior to collection of human tissue. Human adipose tissue was collected in a sterile fashion from the infrapatellar fat pads of patients undergoing total knee arthroplasty. The collected adipose tissue was processed using previously published protocols to obtain the stromal vascular fraction (SVF).<sup>5,17</sup> The resulting SVF was resuspended with growth medium (Dulbecco's modified eagle medium [DMEM; Corning, Corning, NY] containing 10% fetal bovine serum [Gibco, Amarillo, TX] and an antibiotic-antimycotic mix containing 100 unit/ml penicillin, 100 µg/ml streptomycin, and 250 ng/ml amphotericin B [Lonza, Basel, CH]), and expanded in culture. Cells were maintained at 37°C and 5% CO<sub>2</sub>. At passage 1, cells were collected and stored in commercial cell freezing media (Bambanker, GC Lymphotech, Tokyo, Japan) at -80°C until time of use. Frozen cells were later thawed in a 37°C incubator and expanded to reach passage 3.

### 2.2 | Lentiviral transduction

Adipose-derived stem cells were transduced with a two-step transcriptional amplification (TSTA) vector system, as described in previously published protocols.<sup>18-20</sup> Briefly, the TSTA system requires co-transduction of two lentiviral vectors (LV): the GAL4-VP16 transactivator vector and the transgene expression vector, which encodes the G5 promoter and BMP-2 transgene. Passage 3 ASCs were plated at a density of  $1 \times 10^6$  cells/dish. The following day they were transduced in the presence of 8 µg/ml of polybrene with the TSTA vector system (LV-BMP-2) at a multiplicity of infection of 3 for each vector. The cells were incubated overnight and the next day the media was aspirated and replaced with fresh media to remove extracellular virus.

### 2.3 | Cell seeding

Commercially available collagen/biphasic calcium phosphate scaffolds (Mastergraft, Medtronic) were prepared in a sterile fashion and cut to  $6 \times 3 \times 3$  mm. The dimensions of the scaffold were chosen based on the size of an established rat critical size femoral defect model. Using this model and the scaffold described above, our lab has observed reliable bone healing using a minimum of  $5 \times 10^6$  LV-BMP-2 ASCs with a static cell-pipetting technique.<sup>21</sup> Thus, suspensions of 1, 3, or 5 million transduced ASCs were prepared and seeded onto scaffolds using one of three techniques (static, negative pressure, or orbital shaking) described below ( $n = 5$  per seeding method per group). These techniques were adapted from methods previously described by Wang et al. and Melke et al. (Figure 1).<sup>8,15</sup> For our static and negative pressure groups, an equal volume of 40 µl was used per cell suspension, chosen based on prior experience with static pipetting of MSCs onto this scaffold in our lab. In the orbital shaking group, cells were resuspended in 4 ml of growth media as described by Melke et al.<sup>8</sup>

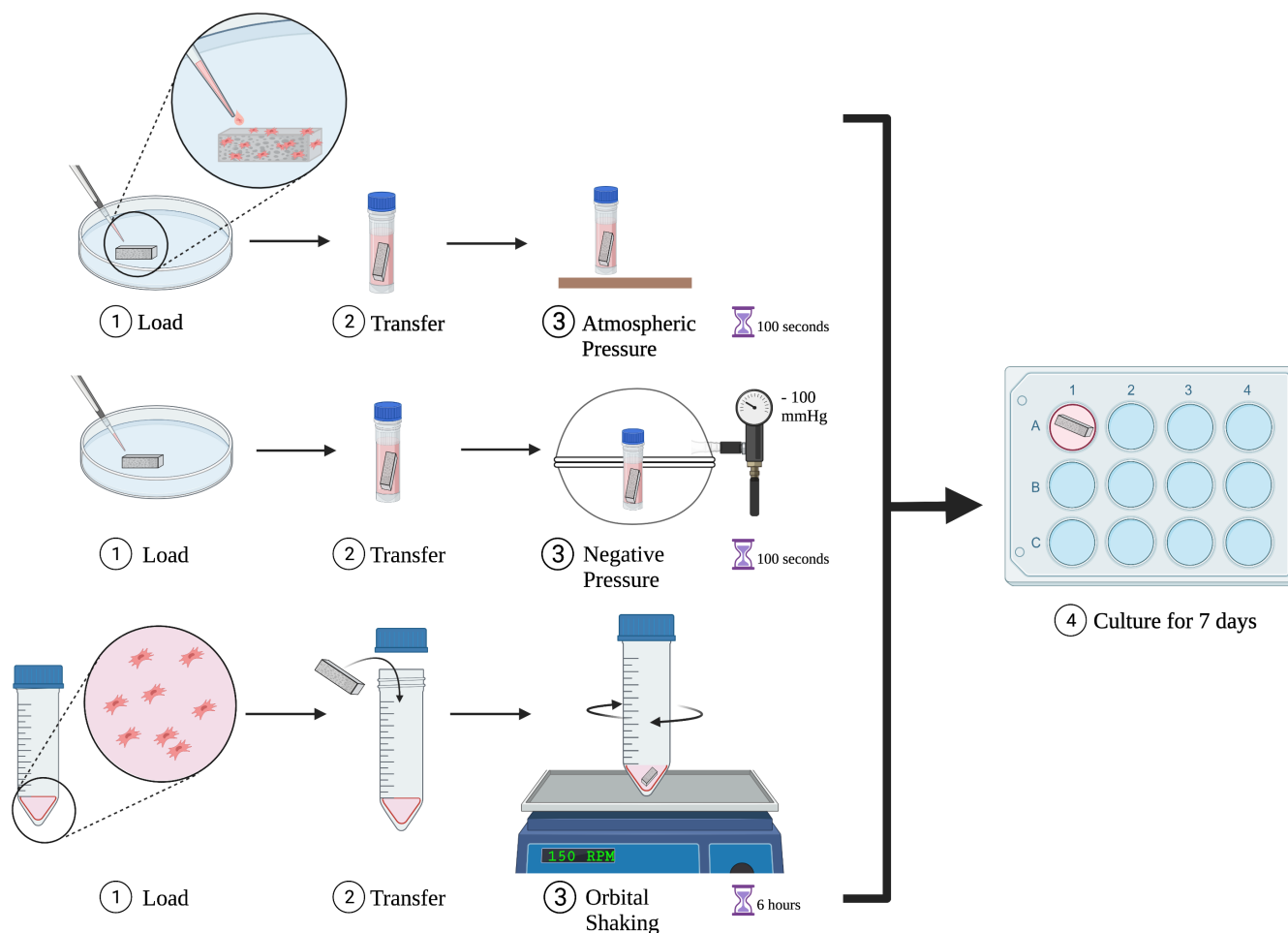


**FIGURE 1** Overview of the static and dynamic cell seeding techniques evaluated. From top to bottom: (1) static (micropipette); (2) negative pressure; and (3) orbital shaking (Created with BioRender.com)

## 2.4 | Group 1—Static seeding

The scaffold was placed in a 10 cm tissue culture dish. Transduced ASCs were resuspended in PBS to a total volume of 40  $\mu$ l and pipetted onto all surfaces of the scaffold using a micropipette. The scaffold was then placed in a 2 ml cryovial containing 500  $\mu$ l of PBS and held at atmospheric pressure for 100 s. Afterwards, the scaffold was transferred to a 12-well plate containing 2 ml of standard growth media per well, and was then cultured at 37°C and 5% CO<sub>2</sub> for 7 days with regular media changes.

## 2.5 | Group 2—Negative pressure seeding

For the negative pressure group, static loading was first performed as described above. After placing scaffolds in 2 ml cryovials containing 500  $\mu$ l PBS, cryovials were then transferred to a vacuum desiccator and negative pressure (−100 mm Hg) was applied for 100 s, as described by Wang et al.<sup>15</sup> The scaffolds were then placed in a

12-well plate containing 2 ml of standard growth media per well and cultured as above.

## 2.6 | Group 3—Orbital shaker seeding

Transduced ASCs were re-suspended in 4 ml of standard growth media and added to a 50 ml centrifuge tube containing the scaffold. The tube was lightly capped and subsequently placed on an orbital shaker set to 150 rpm for 6 h in an incubator at 37°C and 5% CO<sub>2</sub>. After 6 h, the scaffold was transferred to a 12-well plate containing 2 ml of standard growth media and placed in static culture as described above.

## 2.7 | Seeding efficiency

After cell seeding and scaffold transfer to a 12-well plate, the residual cell suspension was examined by cell viability assay using trypan blue and a TC20™ automated cell counter (BioRad, Hercules, CA).

The difference between the total cells applied and the residual cells remaining in solution was used to determine cell seeding efficiency.

## 2.8 | Live cell distribution

Live cell distribution in the scaffold was assessed 24 h after seeding using MTT (3-(4,5-Dimethylthiazol-2-yl)-2,5-Diphenyltetrazolium Bromide) staining and stereo microscopy, similar to the methods described by Wendt et al.<sup>9</sup> Briefly, the cultured scaffolds were gently washed three times with PBS to remove growth media. Scaffolds were subsequently transferred to 3 ml of 0.12 mM MTT solution and incubated for 2 h at 37°C and 5% CO<sub>2</sub>. Afterwards, scaffolds were removed from MTT solution and embedded in a paraffin block for cutting. Stained scaffolds were then bisected and the scaffold cross-sections were imaged at 6× magnification under stereo microscopy and analyzed in ImageJ (NIH) to determine cell penetration into the scaffold. ImageJ color threshold analysis was used to select the “cell-covered” surface area (in mm<sup>2</sup>) and the average greyscale of the selected area was calculated.

The MTT assay measures cellular metabolic activity and can be used as an indicator of cell viability. Therefore, a darker stain, as measured by greyscale values, was taken to represent a higher number of cells per unit area or a higher “cell density.” In ImageJ, a darker stained area corresponds to a lower greyscale, thus the inverse of the greyscale value was multiplied by the area to determine a measurement representative of “total cell number” within the analyzed scaffold cross-section. A detailed description of the methods used for qualitative cell penetration analysis is provided in Figure S1.

To determine “cell penetration” (CP), an “inner core” was drawn using pixel dimensions such that the area of the “inner core” is exactly

half the total area of the scaffold cross-section as shown in Figure 2. After excluding the periphery, color threshold analysis was performed as previously described to provide area and average greyscale values, with subsequent determination of “cell number” present specifically in the “inner core.” To represent the extent of “cell penetration” of the scaffold, the “inner core” cell number was divided by the total cell number to provide the fraction of cells within the scaffold cross-section that penetrated to the “inner core.” As an example, a CP of 0.5 would indicate that half the cells in the scaffold cross-section were found in the “inner core” and half were found in the periphery, indicating a homogenous distribution of cells throughout the scaffold (Figure 2).

## 2.9 | In vitro BMP-2 production

Production of BMP-2 was measured from supernatant collected at 2 and 7 days post-transduction (i.e., 1 or 6 days after cell seeding). The amount of BMP-2 production was quantified by a commercial BMP-2 ELISA kit (Quantikine, R&D systems, Minneapolis, MN). Production was standardized based on donor-matched control cells that were transduced under identical conditions and maintained in culture.

## 2.10 | Scanning electron microscopy (SEM)

After 2 days in culture, one sample from each group underwent fixation and dehydration according to an established protocol. Following dehydration, the samples were frozen in a cryo-fracture chamber and sectioned. Samples were then mounted on SEM stubs and images were collected at 2 keV on a Nova Nano SEM 450 (FEI Company,

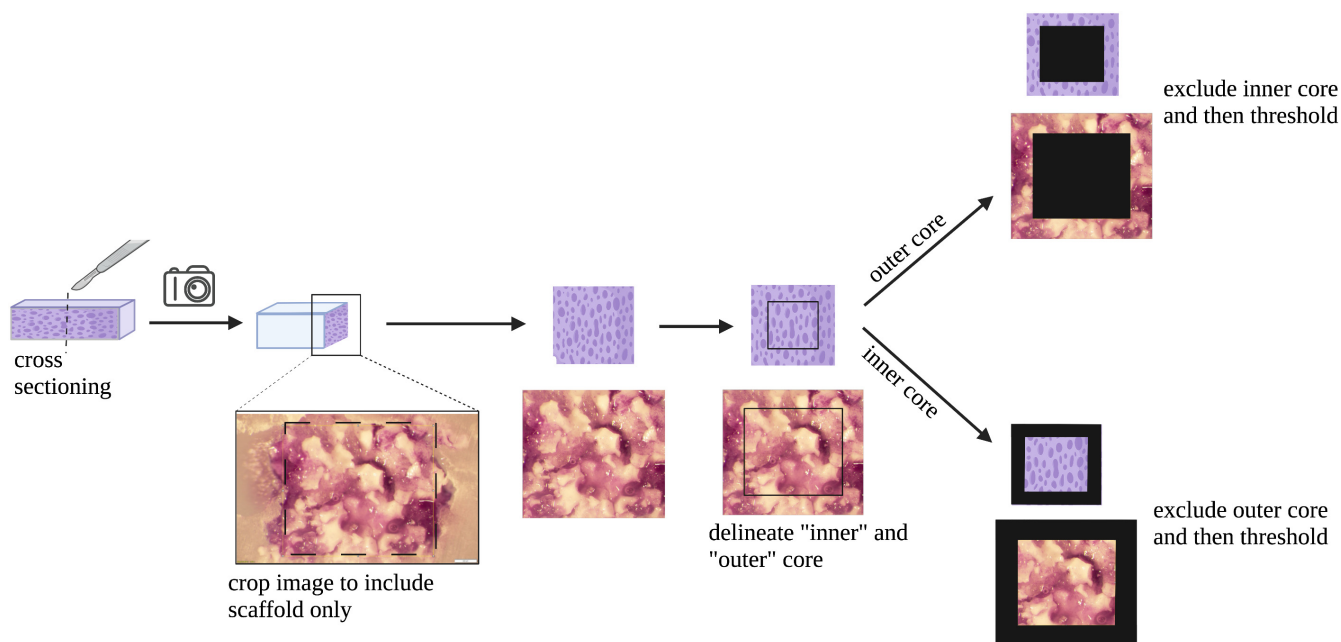


**FIGURE 2** Schematic representation for determining live cell distribution of MTT stained porous scaffold. Scaffolds were sectioned and imaged at 6× using stereo microscopy. Images were then analyzed using ImageJ software to determine the intensity of MTT (purple) staining in the inner and outer halves of the scaffold

**TABLE 1** Comparison of cell seeding methods at 1, 3, and 5 million cells

	Static (S) Mean (SD) N = 5	Negative pressure (NP) Mean (SD) N = 5	Orbital (O) Mean (SD) N = 5	ANOVA or Kruskal–Wallis p value	Significant post hoc Groups <sup>f</sup>
<b>1 × 10<sup>6</sup></b>					
Seeding efficiency <sup>a</sup>	95.5 (2.4)	92.1 (6.1)	58 (7.9)	<.001	S > O; NP > O
Cell penetrance <sup>b</sup>	0.6 (0.02)	0.57 (0.08)	0.53 (0.12)	.45	N/A
Total BMP-2 (2 day) <sup>c</sup>	81.5 (24.0)	63.1 (28.1)	138.0 (8.6)	<.001	O > S; O > NP
Total BMP-2 (7 day) <sup>c</sup>	568.5 (124.6)	692.3 (220.9)	634.6 (59.8)	.45	N/A
Total BMP % increase <sup>d</sup>	614.5 (79.3)	1054.9 (188.0)	360.0 (31.9)	<.001	NP > S > O
BMP per 1 × 10 <sup>6</sup> seeded cells <sup>e</sup>					
2 day total	86.6 (24.7)	65.0 (29.2)	217.0 (12.6)	<.001	O > S; O > NP
7 day total	604.8 (127.2)	713.3 (234.4)	996.6 (62.9)	.006	O > S; O > NP
<b>3 × 10<sup>6</sup></b>					
Seeding efficiency <sup>a</sup>	90.5 (3.7)	88.3 (5.3)	51.3 (20.9)	<.001	S > O; NP > O
Cell penetrance <sup>b</sup>	0.44 (0.05)	0.45 (0.09)	0.47 (0.05)	.77	N/A
Total BMP-2 (2 day) <sup>c</sup>	312.5 (31.3)	372.8 (91.9)	207.3 (11.4)	.01	NP > O
Total BMP-2 (7 day) <sup>c</sup>	743.5 (149.0)	1042.8 (160.8)	732.2 (113.9)	.01	NP > S; NP > O
Total BMP % increase <sup>d</sup>	136.2 (29.4)	188.6 (63.2)	252.0 (40.4)	.01	O > S
BMP per 1 × 10 <sup>6</sup> seeded cells <sup>e</sup>					
2 day total	116.9 (14.1)	138.4 (36.3)	203.1 (76.8)	.048	O > S
7 day total	278.9 (63.5)	384.8 (46.4)	722.9 (296.2)	.005	O > S; O > NP
<b>5 × 10<sup>6</sup></b>					
Seeding efficiency <sup>a</sup>	75 (8.3)	84 (3.4)	28.6 (12.3)	<.001	NP > S > O
Cell penetrance <sup>b</sup>	0.4 (0.12)	0.48 (0.07)	0.42 (0.16)	.55	N/A
Total BMP-2 (2 day) <sup>c</sup>	451.0 (52.5)	437.1 (67.1)	233.4 (40.6)	<.001	S > O; NP > O
Total BMP-2 (7 day) <sup>c</sup>	1060.8 (90.0)	1011.4 (89.0)	817.8 (248.5)	.2	N/A
Total BMP % increase <sup>d</sup>	137.3 (28.8)	136.3 (46.0)	247.5 (71.7)	.007	O > S; O > NP
BMP per 1 × 10 <sup>6</sup> seeded cells <sup>e</sup>					
2 day total	129.5 (18.8)	102.4 (14.9)	200.0 (88.1)	.03	O > NP
7 day total	303.9 (32.5)	238.0 (30.0)	663.6 (212.8)	.004	O > S > NP

<sup>a</sup>Value shown represents the % of seeded cells that successfully adhered to the scaffold.

<sup>b</sup>Calculated ratio of cells that penetrated scaffold inner core.

<sup>c</sup>Adjusted BMP-2 production, units in ng.

<sup>d</sup>Calculated as % increase from day 2 to day 7.

<sup>e</sup>Adjusted BMP-2 production per 1 × 10<sup>6</sup> seeded cells.

<sup>f</sup>NP, negative pressure; O, orbital; S, standard.

Thermo Fisher Scientific, Hillsboro, OR). Images were collected at the center of the sectioned face, and at the periphery of each sample. Selected images were false colored using Photoshop. Detailed methods for SEM imaging are available in the supplemental materials.

test with post-hoc testing adjusted by the Bonferroni method. Analysis was performed for groups stratified by seeding method and by cell density. The level of significance was set at  $p < .05$ . All analyses were performed in SPSS v28.0 (IBM Corp., Armonk, NY).

### 3 | STATISTICAL ANALYSIS

For each loading condition at each cell density, data are presented as the mean ± standard deviation. Normality of the data were confirmed with the Shapiro–Wilk test and homogeneity of variance was confirmed by the Levene test. Between group means were compared with one-way analysis of variance (ANOVA) followed by Tukey's HSD, Welch ANOVA followed by Games-Howell tests, or Kruskal–Wallis

### 4 | RESULTS

#### 4.1 | Effect of cell seeding method on seeding efficiency

At a cell loading density of 1 M, static seeding and dynamic seeding with negative pressure both resulted in high seeding efficiencies (>90%). These methods were significantly more efficient compared to

**TABLE 2** Comparison of cell density with static seeding, negative pressure, and orbital seeding

	$1 \times 10^6$ Mean (SD) N = 5	$3 \times 10^6$ Mean (SD) N = 5	$5 \times 10^6$ Mean (SD) N = 5	ANOVA, Welch or Kruskal–Wallis p value	Significant post hoc Groups <sup>f</sup>
<b>Static seeding</b>					
Seeding efficiency <sup>a</sup>	95.5 (2.4)	90.5 (3.7)	75 (8.3)	<.001	1 > 3 > 5
Cell penetrance <sup>b</sup>	0.6 (0.02)	0.44 (0.04)	0.4 (0.12)	<.001	1 > 3; 1 > 5
Total BMP-2 (2 day) <sup>c</sup>	81.5 (24.0)	312.5 (31.1)	451.0 (52.5)	<.001	5 > 3 > 1
Total BMP-2 (7 day) <sup>c</sup>	568.5 (124.6)	743.5 (149.0)	1060.8 (90.0)	<.001	5 > 1; 3 > 1
Total BMP % increase <sup>d</sup>	614.5 (79.3)	136.2 (29.4)	137.3 (28.8)	<.001	1 > 3; 1 > 5
BMP per $1 \times 10^6$ seeded cells <sup>e</sup>					
2 day total	86.6 (24.7)	116.9 (14.1)	129.5 (18.8)	.01	5 > 1
7 day total	604.8 (127.2)	278.9 (63.5)	303.9 (32.5)	.005	1 > 3; 1 > 5
<b>Negative pressure</b>					
Seeding efficiency <sup>a</sup>	92.1 (6.1)	88.3 (5.3)	84 (3.4)	.005	1 > 5
Cell penetrance <sup>b</sup>	0.57 (0.08)	0.45 (0.09)	0.48 (0.07)	.08	N/A
Total BMP-2 (2 day) <sup>c</sup>	63.1 (28.1)	372.8 (91.9)	437.1 (67.1)	.004	5 > 1
Total BMP-2 (7 day) <sup>c</sup>	692.3 (220.9)	1042.8 (160.8)	1011.4 (89.0)	.01	3 > 1; 5 > 1
Total BMP % increase <sup>d</sup>	1054.9 (188.0)	188.6 (63.2)	136.3 (46.0)	<.001	1 > 3; 1 > 5
BMP per $1 \times 10^6$ seeded cells <sup>e</sup>					
2 day total	65.0 (29.2)	138.4 (36.3)	102.4 (14.9)	.006	3 > 1
7 day total	713.3 (234.4)	384.8 (46.4)	238.0 (30.0)	<.001	1 > 3; 1 > 5
<b>Orbital</b>					
Seeding efficiency <sup>a</sup>	58.0 (7.9)	51.3 (20.9)	28.6 (12.3)	<.001	1 > 5; 3 > 5
Cell penetrance <sup>b</sup>	0.53 (0.12)	0.47 (0.05)	0.42 (0.16)	.42	N/A
Total BMP-2 (2 day) <sup>c</sup>	138.0 (8.6)	207.3 (11.4)	233.4 (40.6)	<.001	3 > 1; 5 > 1
Total BMP-2 (7 day) <sup>c</sup>	634.6 (59.8)	732.2 (113.9)	817.8 (248.5)	.22	N/A
Total BMP % increase <sup>d</sup>	360.0 (31.9)	252.0 (40.4)	247.5 (71.7)	.01	1 > 3; 1 > 5
BMP per $1 \times 10^6$ seeded cells <sup>e</sup>					
2 day total	217.0 (12.6)	203.1 (76.8)	200.0 (88.1)	.92	N/A
7 day total	996.6 (62.9)	722.9 (296.2)	663.6 (212.8)	.06	N/A

<sup>a</sup>Value shown represents the % of seeded cells that successfully adhered to the scaffold.

<sup>b</sup>Calculated fraction of cells loaded that penetrated scaffold inner core.

<sup>c</sup>Adjusted BMP-2 production, units in ng.

<sup>d</sup>Calculated as % increase from day 2 to day 7.

<sup>e</sup>Adjusted BMP-2 production per  $1 \times 10^6$  seeded cells.

<sup>f</sup>Millions of cells loaded.

dynamic seeding with orbital shaking over a period of 6 h (<60%). We observed the same associations between seeding methods and seeding efficiency at cell loading densities of 3 and 5 M ( $p < .001$  for all comparisons, Table 1).

## 4.2 | Effect of cell seeding method on cell distribution

At cell loading densities of 1, 3, and 5 M, we did not observe significant differences in cell penetrance (CP) between the three seeding methods (Table 1). All three methods showed a relatively homogenous cell distribution throughout the scaffold volume (CP ranged from 0.4

to 0.6, with a CP of 0.5 representing an equal number of cells in the inner and outer halves of the scaffold).

## 4.3 | Effect of cell seeding method on BMP-2 transgene expression

In scaffolds loaded with 1 M cells, total BMP-2 production at 2 days post-transduction was significantly higher in the orbital shaking group compared to negative pressure or static seeding ( $p < .001$ ), despite significantly lower cell seeding efficiency in this group (58% vs. 95.5% and 92.1%,  $p < .001$ ; Table 1). After 7 days in culture, this difference was no longer statistically significant. In contrast, in scaffolds loaded



with 3 or 5 M cells, total BMP-2 production at 2 and 7 days tended to be higher in the static or negative pressure groups compared to orbital shaking. Because seeding efficiency differed between groups, with orbital shaking demonstrating starkly lower efficiencies, we also performed an analysis to account for seeding efficiency which compared BMP-2 production per 1 M successfully seeded cells. At all three cell densities, the orbital shaking technique demonstrated a significantly higher BMP-2 production *per cell* than either static or negative pressure loading techniques (Table 1).

#### 4.4 | Effect of cell seeding density on seeding efficiency, cell distribution, and BMP-2 expression

Increasing cell seeding density was associated with a lower cell seeding efficiency for all three seeding methods tested ( $p < .001$  for all groups). Cell penetrance also tended to decrease with increasing cell

seeding density; the change in cell penetrance in statically loaded cells was as high as 30% from 1 to 5 M, meaning a higher proportion of cells were accumulated on the outer half of the scaffold when a higher number of cells were seeded (Table 2). This finding was also observed in the SEM images (Figure 3A,B).

Cell seeding density also had a significant effect on BMP-2 production. With all three seeding techniques, the increase in BMP-2 production from day 2 to day 7 (BMP-2% Increase, Table 2) was significantly higher with a seeding density of 1 M cells versus both 3 and 5 M cell densities.

#### 4.5 | Scanning electron microscopy

Cell distribution was qualitatively assessed by scanning electron microscopy of scaffold cross-sections. Figure 3A,B are representative images demonstrating cell clustering and cell-cell adhesions noted at the periphery of scaffolds and decreased cell penetration to the central core of the scaffold when seeded with high density solutions (5 M cells).

## 5 | DISCUSSION

In any cell-based therapy for bone repair, the cells must be loaded on a carrier to ensure that the cells stay in the intended anatomic location; the carrier may also serve as a scaffold to support bone formation. However, determination of an ideal, maximally efficient cell-seeding technique will be critical to optimize this therapy in the clinical setting and minimize both cost and resource expenditure. We have previously shown that the efficiency of *ex vivo* regional gene therapy with human bone marrow-derived stem cells transduced with a lentiviral vector carrying the BMP-2 transgene is influenced by the number of cells implanted in the bone defect: in an immune deficient rat critical sized femoral defect model, there was a 100% union rate with 15 million MSCs, an 86% union rate with 5 million MSCs, and a 43% union rate with the use of 1 million MSCs.<sup>21</sup> Scaling this small animal model to a large animal or human would require exponential increases in MSCs, viral vector and transduction reagent, as well as time and cost. For this reason, there is significant interest in reducing the number of MSCs required in *ex vivo* gene therapy, while still maintaining therapeutic efficacy. Investigations by Hasegawa et al. and Melke et al. have demonstrated increased osteogenic potential and increased cell seeding efficiencies associated with negative pressure and orbital shaking techniques.<sup>8,13</sup> However, these studies evaluated non-transduced cells. Our study used similar cell seeding techniques to identify an optimal cell-seeding strategy with respect to seeding efficiency, cell uniformity, and *in vitro* BMP-2 production of human ASCs transduced with the LV-TSTA-BMP-2 vector and loaded onto collagen/biphasic calcium phosphate scaffolds.

We demonstrate in the present *in vitro* study that seeding efficiency and homogeneity of cell distribution in scaffolds seeded with transduced ASCs are significantly improved by decreasing the density

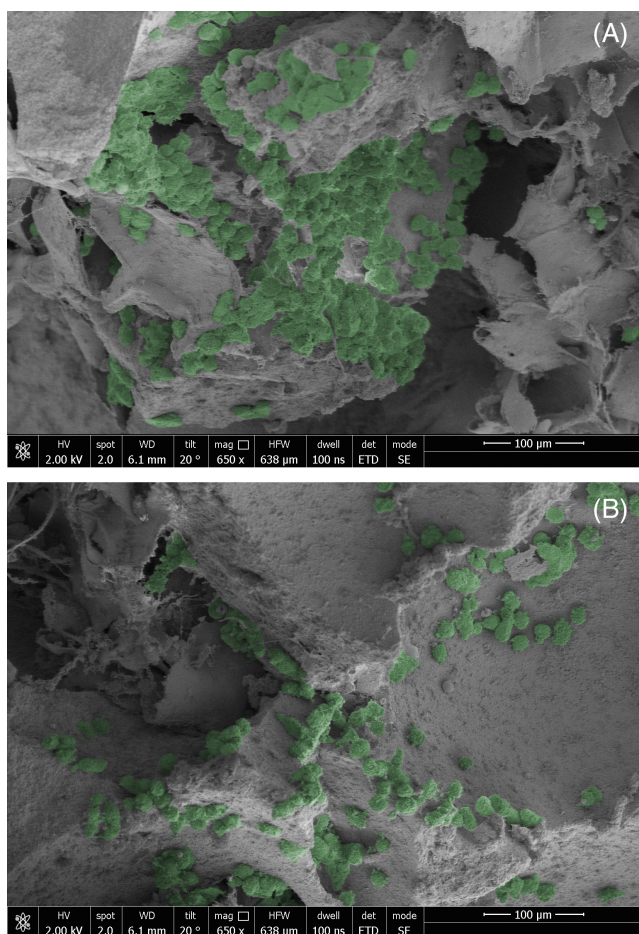


**FIGURE 3** Representative SEM images demonstrating lower cell penetrance with high density cell suspensions due to peripheral clustering of cells (colorized in green). Images were taken at 650 $\times$ . (A) Image taken at scaffold periphery demonstrates cells clustered on TCP granule after loading of 5 M cells using static seeding technique. (B) Image of the same scaffold taken at central core demonstrates TCP granules with sparsely populated cells, indicating poor scaffold penetration

of cell suspensions, and that dynamic seeding by orbital shaking, while exhibiting significantly lower cell seeding efficiency, is associated with increased expression of the BMP-2 transgene. Our results have revealed a potential opportunity to optimize cell seeding of transduced cells for regional gene therapy applications for bone repair by minimizing cell numbers while maintaining comparable levels of BMP-2 expression.

We noted that cell density had an inverse relationship with cell-seeding efficiency in all three seeding methods. There was significant cell clustering with high density cell suspensions in statically loaded constructs (Figure 3), similar to the observations of Griffon et al. with peripherally based sheets of cells in static and spinner flask seeding methods.<sup>22</sup> The increasing cell-cell interaction and adhesions in high density solutions leads to the formation of cell clusters and sheets which likely hinders the ability of individual cells to adhere to and remain on the scaffold, thus decreasing seeding efficiency. Additionally, cell clustering may impair the ability of individual cells to penetrate small pores in the scaffold, thereby decreasing the uniformity of cell distribution, as demonstrated in Figure 3. In support of this theory, we observed in our statically seeded constructs that cell penetration was significantly lower in our highest cell density group. These data suggest that utilization of lower-density cell suspensions, or perhaps the use of more advanced systems such as perfusion bioreactors which rely on continuous dynamic fluid flow, can potentially mitigate this phenomenon.

Negative pressure and static seeding methods demonstrated significantly higher cell seeding efficiency at all cell densities compared to orbital shaking. This finding contrasts with those of Melke et al. who demonstrated significantly higher seeding efficiency of non-transduced human BMSCs seeded with orbital shaking. We observed that even in our low density cell group, which utilized the methods described by Melke et al., the cells had largely settled out of solution at the end of a 6 h culturing period. While we used the same number of cells and identical methods, it is possible that differences between adipose-derived and bone marrow-derived MSCs, as well as differences between transduced and non-transduced MSCs, affect their ability to remain in solution at various densities and dynamic shaking conditions.

With respect to BMP-2 production, there were two critical observations. First, there was a proportional increase in BMP-2 production *per cell* in the orbital shaking group when compared with the static and negative pressure groups. At day 7 post-transduction, the *in vitro* BMP-2 production per cell was significantly higher in the orbital shaking group compared with both static and negative pressure seeding groups. The magnitude of this difference was so great that despite demonstrating only half the seeding efficiency of the static and negative pressure groups when loading 1 M cells, the orbital shaking group produced equivalent levels of *total* BMP-2 at 7 days (Table 1). This suggests that the addition of orbital shaking significantly enhances transgene expression and BMP-2 production, potentially allowing us to achieve equivalent BMP-2 levels with significantly fewer cells. This finding is consistent with prior studies which demonstrate an important role for mechanostimulation in the form of fluid shear stresses in the osteogenic differentiation of MSCs, and supports the use of

dynamic cell seeding methods for transduced cells in *ex vivo* regional gene therapy for bone repair.<sup>23,24</sup>

Additionally, there was a significantly greater increase in BMP-2 production from 2 to 7 days after seeding of 1 M cells when compared to higher cell density suspensions. With all three seeding techniques, the scaffolds loaded with 1 M cells demonstrated significantly greater increases in BMP-2 production from 2 to 7 days, when compared with scaffolds loaded with either 3 or 5 M cells. Over-crowding of cells on the scaffold could potentially inhibit MSC proliferation, or lead to inadequate nutrient uptake from culture media. Additionally, if cells are over-crowded and prone to clustering, this may decrease adhesion and interaction of individual cells with the scaffold material. This could have a negative effect on the osteogenic potential of the transduced cells, as prior studies have demonstrated that MSC-scaffold interaction has important effects on MSC behavior and differentiation potential.<sup>25</sup>

Our study has limitations. First, methods for determining cell-seeding efficiency and cellular uniformity within seeded scaffolds vary widely in the literature and thus there are no fully validated techniques. We used a combination of previously described techniques and adapted these for our specific scaffold composition. Second, our study investigated one specific scaffold material, size, and geometry, and only used transduced human adipose-derived stem cells. It is unclear whether our data can be generalized to other scaffold material and geometry, or cell type. Finally, our study lacks an *in vivo* component to correlate cell-loading conditions with bone formation. However, the present study alone provides invaluable information on the effects of various cell-loading conditions on *in vitro* BMP-2 production, which has been previously demonstrated to directly correlate with *in vivo* bone production in animal models of bone regeneration using gene therapy with BMP-2 producing transduced MSCs.<sup>6,21</sup>

## 6 | CONCLUSIONS

This study is the first to investigate the effect of scaffold seeding methods on transgene expression of transduced MSCs. Our findings suggest that for the successful application of *ex vivo* regional gene therapy for bone repair, optimization of cell density and scaffold loading techniques, as well as the addition of cellular mechanostimulation may play a key role in minimizing the number of MSCs needed through enhanced cell seeding efficiency, uniformity of distribution, and BMP-2 production. These have critical implications for the clinical application of this therapy for larger bone defects to reduce cost and resource requirements. Additional studies are needed to determine optimal combinations of cell seeding techniques and dynamic culturing conditions, and to further investigate their impact on *in vivo* bone formation.

## DISCLOSURES

None of the authors have any relevant disclosures to report.



## ACKNOWLEDGMENTS

The authors would like to thank the Core Center for Excellence in Nano Imaging of USC for their assistance with this project.

## DATA AVAILABILITY STATEMENT

The data that support the findings of this study are available from the corresponding author upon reasonable request.

## ORCID

Kevin Collon  <https://orcid.org/0000-0001-8984-2447>

## REFERENCES

- Alluri R, Song X, Bougioukli S, et al. Regional gene therapy with 3D printed scaffolds to heal critical sized bone defects in a rat model. *J Biomed Mater Res A*. 2019;107(10):2174-2182.
- Alluri R, Jakus A, Bougioukli S, et al. 3D printed hyperelastic “bone” scaffolds and regional gene therapy: a novel approach to bone healing. *J Biomed Mater Res A*. 2018;106(4):1104-1110.
- Ahlmann E, Patzakis M, Roidis N, Shepherd L, Holtom P. Comparison of anterior and posterior iliac crest bone grafts in terms of harvest-site morbidity and functional outcomes. *J Bone Joint Surg Am*. 2002;84(5):716-720.
- Younger EM, Chapman MW. Morbidity at bone graft donor sites. *J Orthop Trauma*. 1989;3(3):192-195.
- Vakhshori V, Bougioukli S, Sugiyama O, et al. Ex vivo regional gene therapy with human adipose-derived stem cells for bone repair. *Bone*. 2020;138:115524.
- Bougioukli S, Alluri R, Pannell W, et al. Ex vivo gene therapy using human bone marrow cells overexpressing BMP-2: “next-day” gene therapy versus standard “two-step” approach. *Bone*. 2019;128:115032.
- Peng H, Wright V, Usas A, et al. Synergistic enhancement of bone formation and healing by stem cell-expressed VEGF and bone morphogenetic protein-4. *J Clin Invest*. 2002;110(6):751-759.
- Melke J, Zhao F, Ito K, Hofmann S. Orbital seeding of mesenchymal stromal cells increases osteogenic differentiation and bone-like tissue formation. *J Orthop Res*. 2020;38(6):1228-1237.
- Wendt D, Marsano A, Jakob M, Heberer M, Martin I. Oscillating perfusion of cell suspensions through three-dimensional scaffolds enhances cell seeding efficiency and uniformity. *Biotechnol Bioeng*. 2003;84(2):205-214.
- Cheng G, Youssef BB, Markenscoff P, Zygorakis K. Cell population dynamics modulate the rates of tissue growth processes. *Biophys J*. 2006;90(3):713-724.
- Xing Z, Xue Y, Danmark S, et al. Comparison of short-run cell seeding methods for poly(L-lactide-co-1,5-dioxepan-2-one) scaffold intended for bone tissue engineering. *Int J Artif Organs*. 2011;34(5):432-441.
- Villalona GA, Udelsman B, Duncan DR, et al. Cell-seeding techniques in vascular tissue engineering. *Tissue Eng Part B Rev*. 2010;16(3):341-350.
- Hasegawa T, Miwa M, Sakai Y, et al. Efficient cell-seeding into scaffolds improves bone formation. *J Dent Res*. 2010;89(8):854-859.
- Thevenot P, Nair A, Dey J, Yang J, Tang L. Method to analyze three-dimensional cell distribution and infiltration in degradable scaffolds. *Tissue Eng Part C Methods*. 2008;14(4):319-331.
- Wang J, Asou Y, Sekiya I, Sotome S, Orii H, Shinomiya K. Enhancement of tissue engineered bone formation by a low pressure system improving cell seeding and medium perfusion into a porous scaffold. *Biomaterials*. 2006;27(13):2738-2746.
- Sauerova P, Suchy T, Supova M, et al. Positive impact of dynamic seeding of mesenchymal stem cells on bone-like biodegradable scaffolds with increased content of calcium phosphate nanoparticles. *Mol Biol Rep*. 2019;46(4):4483-4500.
- Zhu M, Heydarkhan-Hagvall S, Hedrick M, Benhaim P, Zuk P. Manual isolation of adipose-derived stem cells from human lipoaspirates. *J Vis Exp*. 2013;79:e50585.
- Alaee F, Bartholomae C, Sugiyama O, et al. Biodistribution of LV-TSTA transduced rat bone marrow cells used for “ex-vivo” regional gene therapy for bone repair. *Curr Gene Ther*. 2015;15(5):481-491.
- Iyer M, Wu L, Carey M, Wang Y, Smallwood A, Gambhir SS. Two-step transcriptional amplification as a method for imaging reporter gene expression using weak promoters. *Proc Natl Acad Sci U S A*. 2001;98(25):14595-14600.
- Virk MS, Sugiyama O, Park SH, et al. “Same day” ex-vivo regional gene therapy: a novel strategy to enhance bone repair. *Mol Ther*. 2011;19(5):960-968.
- Ihn H, Kang H, Iglesias B, et al. Regional gene therapy with transduced human cells: the influence of “cell dose” on bone repair. *Tissue Eng Part A*. 2021;27(21-22):1422-1433.
- Griffon DJ, Abulencia JP, Ragety GR, Fredericks LP, Chaieb S. A comparative study of seeding techniques and three-dimensional matrices for mesenchymal cell attachment. *J Tissue Eng Regen Med*. 2011;5(3):169-179.
- Sun Y, Wan B, Wang R, et al. Mechanical stimulation on mesenchymal stem cells and surrounding microenvironments in bone regeneration: regulations and applications. *Front Cell Dev Biol*. 2022;10:808303.
- Delaine-Smith RM, Reilly GC. Mesenchymal stem cell responses to mechanical stimuli. *Muscl Ligam Tend J*. 2012;2:169-180.
- Gao C, Peng S, Feng P, Shuai C. Bone biomaterials and interactions with stem cells. *Bone Res*. 2017;5:17059.

## SUPPORTING INFORMATION

Additional supporting information can be found online in the Supporting Information section at the end of this article.

**How to cite this article:** Collon K, Bell JA, Chang SW, et al. Effects of cell seeding technique and cell density on BMP-2 production in transduced human mesenchymal stem cells. *J Biomed Mater Res*. 2022;110(12):1944-1952. doi:[10.1002/jbm.a.37430](https://doi.org/10.1002/jbm.a.37430)